

SOVIET PHYSICS JETP

A translation of the Zhurnal Éksperimental'noi i Teoreticheskoi Fiziki

Editor in Chief—P. L. Kapitza; Associate Editors—M. A. Leontovich, E. M. Lifshitz, S. Yu. Luk'yanov; Editorial Board—É. L. Andronikashvili, K. P. Belov, V. P. Dzhelepov, E. L. Feinberg, V. A. Fock, I. K. Kikoin, L. D. Landau, B. M. Pontecorvo, D. V. Shirkov, K. A. Ter-Martirosyan, G. V. Zhdanov (Secretary).

Vol. 26, No. 4, pp. 693-867

(Russ. Orig. Vol. 53, No. 4, pp. 1177-1504)

April 1968

NATURE OF THREE-STAGE INSTABILITY OF A PLASMA BEAM

M. V. NEZLIN

Submitted January 21, 1967

Zh. Eksp. Teor. Fiz. 53, 1180-1194 (October, 1967)

We investigate experimentally the mechanism of the instability that is responsible for the acceleration (heating) of the ions and the interruption of the current (formation of a virtual cathode) in an electron beam passing through a plasma column. We show that this instability has a three-stage character. The first stage of the instability is connected with flute (centrifugal) instability of a plasma rotating under the influence of an equilibrium radial electric field "crossed" with an external magnetic field. The second and third stages, according to the presented point of view, are connected respectively with the kinetic and hydrodynamic buildups of the drift-beam instability considered theoretically in^[10,11].

INTRODUCTION

WE have previously investigated^[1-3] certain manifestations of instability of a plasma beam in a longitudinal magnetic field: the existence of discrete states of the beam, formation of a virtual cathode in one of these states, and stochastic acceleration of the ions to high energies. The present study with the same experimental setup which was used earlier to investigate the discrete states of a plasma beam^[3]. The main parameters of this setup (1) are as follows: beam diameter (in the stable state) 1 cm, beam length variable from 20 to 150 cm, diameter of vacuum chamber 30 cm, magnetic field homogeneous along the installation and constant in time, from 100 to 8000 Oe, pressure of neutral gas in the plasma-beam source (which was 15 cm long and 2 cm in diameter) $p = p_1 \approx 10^{-4}$ mm Hg, and in the vacuum chamber $p = p_2 \approx 10^{-5}$ mm Hg. p_1 was regulated by varying the flow of the gas (Q) fed to the source. Certain experiments were made at much smaller values of p_1 and p_2 , for example $p_1 = p_2 \approx 1 \times 10^{-6}$ mm mercury (see below).

In accordance with^[3], we assumed it unlikely that the main causes of the beam instability are connected with high-frequency (Langmuir) oscillations. Our efforts were therefore directed towards the study of the evolution of the low-frequency oscillations of the plasma beam while gradually varying those parameters which determine its state. Such parameters are, first of all, the ratio (α) of the plasma density to the density n_1 of the current of fast (primary) electrons, the beam length (L_b), and the magnetic-field intensity. The working gases were argon and nitrogen. The experiments with a plasma beam ($p_1 \gg p_2$) were carried out as a rule

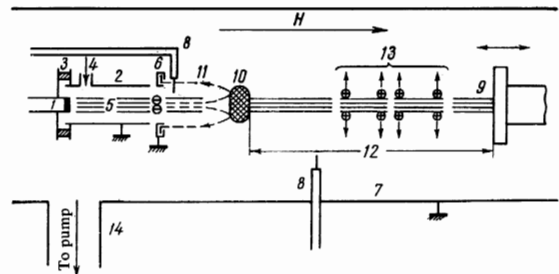


FIG. 1. Experimental setup: 1—cathode of 1 cm diameter, having a negative potential $-V_p$; 2—discharge chamber 2 cm in diameter and 51 cm long, at zero potential; 3—insulator; 4—gas inlet; 5—beam; 6—ring electrode; 7—vacuum chamber; 8—probes; 9—anode; 10—virtual cathode; 11—trajectory of electron beam at the instant of formation of the virtual cathode; 12—region of positive potential; 13—accelerated ion; 14—vacuum.

under identical discharge conditions: discharge current $I_d = 0.5-1$ A and voltage $V_d = 250$ V; the phenomena observed under other conditions were qualitatively the same. The setup for measuring the oscillations was the same as before^[3].

In many cases we used instead of the oscillation amplitude a different indicator of the state of the beam, namely the potential (φ_r) to which an insulated ring electrode (6 in Fig. 1), "looking" at the anode through a narrow slot in the screen, becomes charged by the electrons as it moves opposite to the beam.

The higher this (negative) potential, the more unstable the beam^[3]. At the first stage of the instability (state I) $\varphi_r = 0$, at the second stage (state II) $\varphi_r = -(10-50)$ V, and at the third stage (state III) $\varphi_r \approx -250$ V.

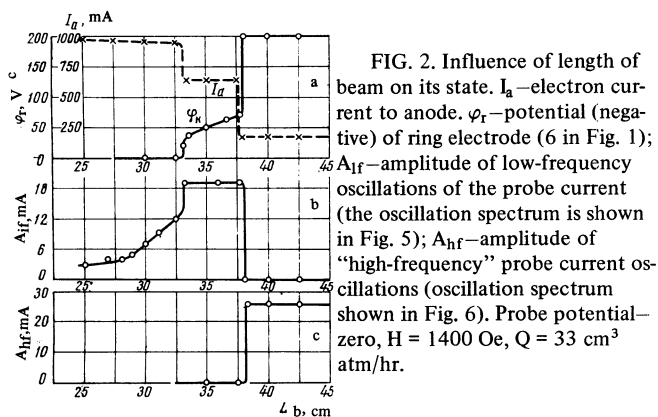


FIG. 2. Influence of length of beam on its state. I_a —electron current to anode. φ_r —potential (negative) of ring electrode (6 in Fig. 1); A_{lf} —amplitude of low-frequency oscillations of the probe current (the oscillation spectrum is shown in Fig. 5); A_{hf} —amplitude of “high-frequency” probe current oscillations (oscillation spectrum shown in Fig. 6). Probe potential—zero, $H = 1400$ Oe, $Q = 33$ cm³ atm/hr.

1. NATURE OF THE INSTABILITY OF STATE I

Figure 2 shows the influence of the beam length L_b (equal to the distance between the cathode and the anode) on the quantities characterizing its state, namely the electron current to the anode I_a , the energy of the electrons moving opposites to the beam ($e\varphi_r$), and the amplitude of the oscillations of the anode current (A_{\sim}). Figure 2a, which is shown to demonstrate the succession of the earlier experimental data, duplicates the previously known results^[3]: 1) if the beam length is smaller than a certain critical length L_{CR} , then the beam is in state I with $\varphi_r = 0$; this state, in which no ion acceleration is observed, was arbitrary defined as stable in^[3]; 2) the jumps in the values of φ_r and I_a correspond to transitions of the beam between the three discrete states I, II and III. Thus, the transition I \rightarrow II takes place when $L_b = L_{CR}$ (in our case $L_{CR} \approx 33$ cm).

It is seen from Fig. 2b that the transition I \rightarrow II is preceded by a strong growth of the anode current oscillations (the frequencies of these oscillations range from several kHz to several dozen kHz—see Fig. 5). In state II these oscillations vary weakly (they reach saturation). At the instant of the transition II \rightarrow III the low-frequency oscillations practically vanish, and are replaced by oscillations with frequency on the order of 300–400 kHz (and its harmonics)—see Fig. 2c. The spectra of these oscillations were investigated earlier^[3], and one of the characteristic spectra is shown in Fig. 6 below. When the gas flow (Q) increases, all the plots shown in Fig. 2 shift towards longer beam lengths. The critical length L_{CR} depends in this case on the direction of the experiment: L_{CR} is larger when the beam length is increased than when it is decreased (hysteresis).

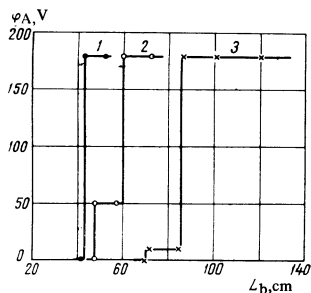


FIG. 3. Potential of ring electrode vs. length of beam in three magnetic fields: 1, 2, 3,— $H = 1000$, 1300, and 1600 Oe, respectively; $Q = 33$ cm³ atm/hr.

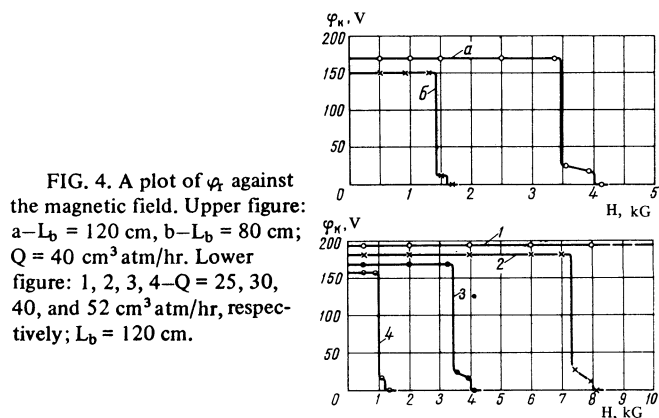


FIG. 4. A plot of φ_r against the magnetic field. Upper figure: a— $L_b = 120$ cm, b— $L_b = 80$ cm; $Q = 40$ cm³ atm/hr. Lower figure: 1, 2, 3, 4— $Q = 25, 30, 40$, and 52 cm³ atm/hr, respectively; $L_b = 120$ cm.

The data of Fig. 2 were obtained in a relatively weak magnetic field ($H = 1400$ Oe). An increase in the magnetic field contributes to the beams stability. This is seen from Figs. 3 and 4. Figure 3 shows that those values of the beam length in which transitions I \rightarrow II and II \rightarrow III take place increase with increasing magnetic field. Figure 4 shows that when the magnetic field is increased, the plasma beam hitherto in the state III ($\varphi_r = -(150-200)$ V) goes through transitions III \rightarrow II and II \rightarrow I. The longer the beam (upper part of Fig. 4) and the lower the pressure (flow) of the gas in the source (lower part of Fig. 4) the larger the magnetic field intensity in which these transitions take place.

The spectra of the low-frequency oscillations whose amplitude growth precedes the transition I \rightarrow II are shown in Fig. 5 for different beam lengths ($L_b < L_{CR}$). We see that the spectrum of the oscillations changes with increasing beam length: the spectrum first becomes “enriched” with harmonics of the fundamental frequency f_0 ($f_0 = 20$ kHz in Figs. 5a–c), and then, when the oscillations are strong, this frequency decreases (Fig. 5d, $f_0 \approx 8$ kHz).

The structure of these oscillations was investigated with the aid of two groups of probes: the probes of one group were located at different points along the beam and had identical radial and azimuthal coordinates, while the probes of the other group were located at different azimuths. Comparison of phases and amplitudes of the signals of these two groups of probes has shown that the oscillations in question are a reflection of the fact that an eccentric flare is ejected from the beam; this flare is homogeneous along the beam and rotates in the “ion” side with a frequency equal to the fundamental oscillation frequency f_0 . In the experiment we have observed constancy of the phase in amplitude of the oscillations along the flare indicates that the latter has a “flute” origin.

The oscillograms of the oscillations in question have the appearance of either a “fence” without gaps, or a “fence” with gaps, or else a more complicated appearance. They are either regular or irregular (“grass”). The period of the regular oscillations is $1/f_0$, while the irregular oscillations have a “period” which varies randomly in time (the frequency range of both types of oscillations is the same).

The experiments have also shown that azimuthal separation of the charges takes place in the flare, there

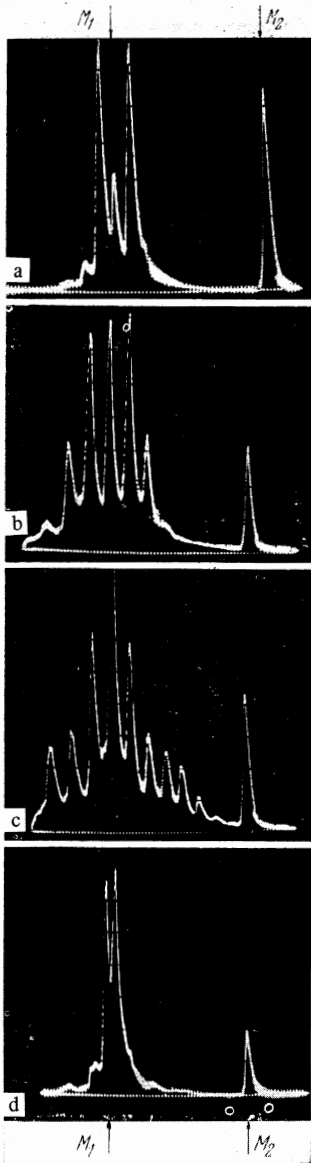


FIG. 5. Spectrum of low-frequency anode-current oscillations at four values of the beam length; a, b, c, d—respectively $L_b = 23, 31, 35,$ and 45 cm; $H = 1300$ Oe; $Q = 45$ cm³ atm/hr; M_1 and M_2 —frequency markers, $f_{M1} = 0$ and $f_{M2} = 200$ kHz.

is an excess of ions on the leading front of the flare, and an excess of electrons in the trailing one. This charge separation produces an azimuthal electric field which causes the flare to grow radially. The longer the beam, the greater the height of the flare (which is approximately the same throughout its length), other conditions being equal. This explains the variation of the oscillations with amplitude in the state I (Fig. 2).

The experimental data allow us to advance the following opinion concerning the nature of the instability of state I. The instability in question is a centrifugal flute instability^[4,5] due to the rotation of the plasma in its own ("internal") radial electric field E_r , crossed with the external longitudinal magnetic field. The internal electric field has a "thermal" origin, and is due to the fact that to retain the electrons, the plasma has a positive potential relative to the (metallic) end surfaces; this potential is on the order of several electron temperatures, T_e/e . Since T_e falls off from the center towards the periphery, the electric field E_r is directed from the center of the beam to the walls; $E_r \approx T_e/eR$,

where R is the "radius" of the plasma^[6]. In the crossed fields E_r and H_z , the plasma rotates at a speed close to cE_r/H_z , and owing to the presence of the centrifugal force, the ions lead the electrons in this rotation. Such a state is unstable, since the density fluctuations lead to an azimuthal distribution of the charges, causing the appearance of an azimuthal electric field E_ϕ ; the particle drift in the crossed fields E_ϕ and H_z produces a plasma flare which increases in the radial direction (and rotates on the ion side).

It is easy to see that this point of view is in good qualitative agreement with the following experimental facts: 1) the presence of a plasma flare and its flute character, 2) the rotation of the flare and the direction of the rotation, 3) the speed of rotation (the experimental order of magnitude of which is cE_r/Az) and the sign of the azimuthal separation of the charges.

According to the foregoing point of view, the larger E_r , that is, the higher T_e , the more unstable the plasma. The value of T_e is determined, on the one hand, by the energy lost by the primary beam to excitation of electronic plasma oscillations, and on the other hand by the rate of escape of plasma electrons from the system. The heating of the plasma electrons by the beam continues until the energy spectrum of the beam assumes the form of a plateau (such a smearing of the spectrum always take place under the conditions of our experiments, even in the state I^[1]). By that instant of time, as is well known^[7], the beam has time to transfer to the plasma electrons the greater part of its initial energy; the smaller the plasma-particle density n_2 , the larger the fraction of the energy transferred per particle. It is therefore natural to expect T_e to increase with decreasing n_2 . (It is assumed that n_2 is sufficiently high, for if n_2 is too small, there will be no time for the plateau to be formed over the length of the beam¹⁾.) This agrees with the experimental data. According to this point of view, the stabilizing influence of the gas flow Q is perfectly understandable, for the larger Q the higher n_2 .

Let us proceed now to explain the dependence of the beam stability on its length and on the intensity of the magnetic field. The criterion for flute centrifugal instability of a plasma situated in a radial electric and longitudinal magnetic field and "frozen" in the metallic end electrodes is^[4,5]:

$$\frac{\pi}{16} \frac{H^2}{L_b^2 n_2 M} < \frac{g}{l}, \quad (1)$$

where L_b is the length of the beam, l the dimension of the disturbance in the direction perpendicular to the plasma boundary, M the ion mass, and g the acceleration due to the force causing the charge separation, in our case the centrifugal force:

$$g = c^2 E_r^2 / RH^2, \quad (2)$$

where R is the plasma radius and $E_r \approx T_e/eR$.

With (2) taken into account, condition (1) becomes

$$\frac{H^4 R^3}{L_b^2 T_e^2 n_2} < 5 \frac{Mc^2}{e^2 l}. \quad (3)$$

¹⁾When speaking of a plasma beam, we have in mind the case of a sufficiently large n_2 , when the condition (9) for the "ignition of the discharge" is satisfied.

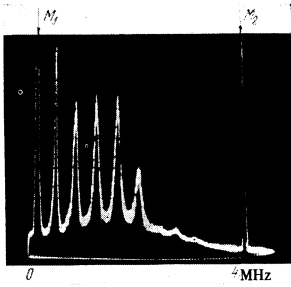


FIG. 6. Spectrum of high-frequency oscillations of probe current in state III. Probe radius 1.5 cm; M_1 and M_2 —frequency markers, $f_{M1} = 0$ and $f_{M2} = 4$ MHz; $Q = 35 \text{ cm}^3 \text{ atm/hr}$, $H = 1400 \text{ Oe}$, $L_b = 150 \text{ cm}$.

Account must be taken here of the fact that, as shown by measurements, $T_e^2 n_2$ decreases with increasing n_2 . Taking this circumstance into account, we see from (3) that the instabilities contribute to an increase of L_b and T_e , and to a decrease of H and n_2 .

It is easy to see that these theoretical predictions are in good qualitative agreement with experiment (Figs. 2–4). Among the factors stabilizing the instability in question, notice should be taken of the smearing of the plasma boundary (increase of the dimension l) and of effects connected with the finite Larmor radius of the ions and the inhomogeneity of the electric field^[8,4].

It should be noted that the destabilizing influence of the beam length is apparently produced also by another mechanism: if the beam is long, the ions have time to diffuse across the magnetic field to larger distances during the time that they move from the plasma source to the anode. That is to say, when the beam is longer the transverse dimension of the flare increases, and the plasma density in the region of the primary beam decreases.

We note also the following experimental fact: the critical length of the beam, which has a smaller diameter ($2a \approx 5 \text{ mm}$ in place of 10 mm) turns out to be smaller, and this also corresponds with criterion (3). Symptoms of centrifugal instability are observed also in states II and III. In particular, we are inclined to attribute to the influence of an “admixture” of such an instability the line part of the oscillation spectrum shown in Fig. 6, which also corresponds to rotation of the flute flare around the beam axis on the ion side. (However, the continuous part of this spectrum is apparently connected with other phenomena, which will be considered in the next section).

2. NATURE OF INSTABILITIES CAUSING THE TRANSITIONS I → II AND II → III

It is easy to see that the instability responsible for the transition I → II differs from that (centrifugal) instability which develops in state I. This follows essentially from two facts. First, in state II we observe ion acceleration ($\perp H$) to high energies—on the order of the energies of the primary electrons of the beam (W_1), that is, larger by dozens of times than the energies of the ions in state I; at the same time, as can be seen from Fig. 2, the amplitude of the (centrifugal) oscillations in the I → II transition increases only insignificantly. Second, in order for the plasma ion to acquire an energy ($\perp H$) on the order of W_1 , it must be accelerated many times, since the amplitude of the oscillations of the ion-accelerating potential is of the order of T_e/e , that is, it

is small compared with W_1/e . However, in the centrifugal instability connected with the equilibrium radial electric field $E_r \approx T_e/eR$, multiple acceleration of the ions (to energies $\approx W_1 \gg T_e$) is impossible. In fact, the electric field produced in the centrifugal instability due to such a field changes at frequencies on the order of the drift frequency, that is, much lower than the Larmor frequencies of the ions (see above), and therefore the transverse ion energy W_\perp remains an adiabatic invariant^[4]. Thus, already in state II (and apparently in state III) the ion acceleration is due to causes not connected with the centrifugal instability.

To attempt to understand these causes, we call attention to the following analogy. A situation wherein ion acceleration takes place in two states of the beam, one of which is furthermore characterized by the occurrence of a virtual cathode in the current of the primary electrons, was observed by us also in experiments^[9] with an electron beam propagating in vacuum. The conditions of such experiments differ from the conditions of the experiments with the plasma beam in that no gas is fed to the source ($Q = 0$), and therefore the density of the primary beam electrons is smaller by about two orders of magnitude. In view of the relative simplicity of these experiments, we shall stop to detail there results, after which we shall consider the connection between these results and the phenomena causing the transitions of the plasma beam between these states I, II and III.

Our experiments have shown that in an electron beam compensated by ions oscillations occur in the frequency range $\sim 100\text{--}500 \text{ kHz}$ (see Figs. 10 and 11). Simultaneously with these oscillations, the ions are accelerated ($\perp H$) to energies that are comparable, if the magnetic fields are not too weak, with the energies of the beam electrons (the ion-energy measurement procedure was the same as before^[2]). Figure 7 shows the dependence of the amplitude of these electron-ion oscillations and the ion energies (W_\perp) on the beam current (the quantity W_\perp is equal to the potential to which the collector of the analyzer used in^[2] is charged by the ions). We see that both relations are well correlated with each other.

Thus, in the case shown in Fig. 7, three discrete states are distinctly separated in the beam: the first—when $I < I_{\text{exc}}$, when there are no electron-ion oscillations and the ion energy is close to zero, the second when $I_{\text{exc}} < I < I_l$, and the electron-ion oscillations lead to an intense acceleration of the ions, and the third

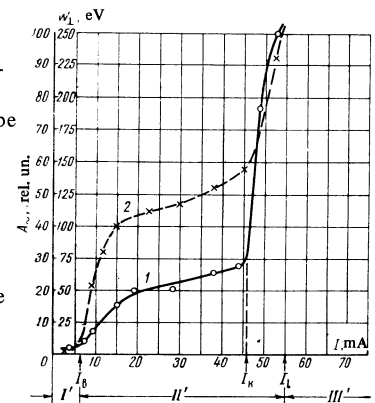


FIG. 7. Dependence of amplitude of electron-ion oscillations of the current to the probe A_\sim (curve 1) and the ion energy W_\perp (curve 2) on the beam current. $W_1 = 300 \text{ eV}$, $H = 200 \text{ Oe}$, $L_b = 100 \text{ cm}$, $p = 2 \times 10^{-6} \text{ mm Hg}$, anode potential $V_a = +100 \text{ V}$, I_{cr} —current at which the oscillation amplitude begins to increase rapidly, I_l —limiting beam current (see also Fig. 11).

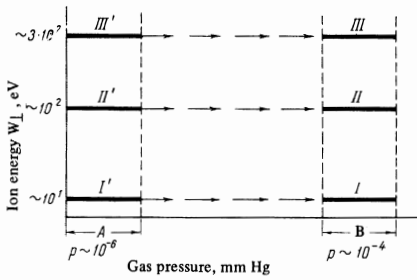


FIG. 8. Illustrative scheme of the "energy levels" of the ions in a vacuum beam (A) and a plasma beam (B).

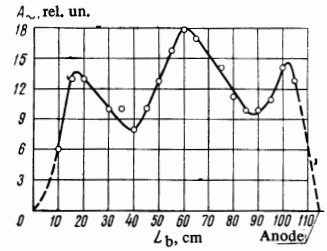
when $I > I_l$, and we have not only ion acceleration but also formation of a virtual cathode in the current of the primary electrons. We shall denote these states by I' , II' , and III' . The analogy indicated above consists in the fact that in this case, just as in the case of a plasma beam, intense ion acceleration occurs only in two states (II' and III'), of which one (III') is additionally characterized by formation of a virtual cathode in the primary beam (the oscillation spectra in states II' and III' are shown in Fig. 11).

Further evidence of the existence of a deep analogy between the discrete states of a plasma beam and a quasineutral electron beam in vacuum is afforded by an experiment performed by us, in which a smooth transition from the electron beam into a plasma beam²⁾ was effected by gradually increasing the gas pressure from $p \approx 1 \times 10^{-6}$ mm Hg to $p \approx 1 \times 10^{-4}$ mm Hg (when condition (9) for the formation of a plasma beam begins to be satisfied). This experiment has shown that three modes of such a transition are possible. If the beam current is kept, during the time that the gas pressure is increased between the indicated limits, so high that $I > I_l$ (in spite of the fact that in this case experiment has shown that I_l increases smoothly by several times), then the continuous transition $III' \rightarrow III$ is effected. In the second mode, when $I_{exc} < I < I_l$, a continuous $II' \rightarrow II$ transition is produced. Finally, when $I < I_{exc}$, the state I' goes over continuously into state I . These transitions are shown schematically in Fig. 8. (It must be noted here that the centrifugal instability considered above exists also in the state I' , but it arises when the gas pressure is not too low, since, in accordance with the criterion (3), the plasma density should exceed a certain minimum value.)

Let us explain a few essential details concerning the transitions from the electron beam to plasma beam. Let us take, for example, the transition $II' \rightarrow II$. In the course of this transition (that is, when the plasma density and the beam current are increased) the spectrum of the oscillations in state II broadens gradually and shifts towards higher frequencies (this can already be seen from Figs. 10 and 11). In addition, starting with a certain plasma density—in connection with the appearing centrifugal instability—low frequencies, the order of several dozen kHz, begin to appear in the spectrum of the oscillations. Therefore, by the time the electron beam is transformed into a plasma beam, the frequency

²⁾In this experiment, that edge of the source discharge chamber which faces the cathode was covered with a grid of tungsten wire of 0.2 mm diameter; the grid was necessary to obtain a sufficiently dense beam in those modes for which conditions (9) was not satisfied.

FIG. 9. Distribution of amplitudes of probe-current oscillations A_{\sim} along the beam. $W_1 = 150$ eV, $L_b = 105$ cm, $H = 1300$ Oe, $p = 3 \times 10^{-6}$ mm Hg.



spectrum of the oscillations (state II) turns out to be, first, strongly smeared out—up to several MHz and even farther³⁾ and, second, it contains an appreciable "admixture" of low frequencies corresponding to the centrifugal instability. Approximately similar changes occur also in the $III' \rightarrow III$ transition. However, inasmuch as the equilibrium radial electric field in the state III is much stronger than in II , the centrifugal instability develops at a much higher frequency—on the order of hundreds of kHz (see Fig. 6).

It must also be emphasized that the transitions $II' \rightarrow II$ and $III' \rightarrow III$ are observed only in the case when a sufficiently large longitudinal pressure drop of the neutral gas ($p_1 \gg p_2$) is maintained between the region of the source and the remaining part of the beam. The influence of the longitudinal pressure gradient on the plasma stability is discussed in Sec. 3.

Thus, the instabilities determining the existence of different discrete states of an electron or plasma beam is apparently based on a common physical mechanism. The nature of this mechanism is additionally characterized by the following experimental data.

First, it was shown in⁹⁾ that the laws governing the interruption of the current in an electron beam (i.e., the character of the dependence of the limiting current I_l on the beam velocity and on the magnetic field intensity) agree well with the theory^[10,11] of the drift-beam instability³⁾. According to this theory, the transition $II' \rightarrow III'$ can be attributed to the fact that when $I > I_{CR} \approx I_l$ there takes place a hydrodynamic buildup of axially asymmetrical electron-ion oscillations, which have a periodic structure along the magnetic field and which propagate around the beam axis on the "electron" side; the frequencies of these oscillations lie in the range

$$\omega_{Hi} < \omega < k_z u, \tag{4}$$

where ω_{Hi} is the Larmor frequency of the ions, u is the velocity of the (monoenergetic) beam, and k_z is the longitudinal wave number ($k_z = 2\pi/\lambda_z$).

Second, our experiments have shown that electron-ion oscillations possessing these properties are indeed observed in the state II' . These experiments were made with the aid of disc probes of 1 cm diameter, arranged on a radius of 5 cm—both along the magnetic field (20 probes) and around the beam axis (3 probes). The results of these experiments are shown in Figs. 9–11.

The first of these figures shows the distribution of the electron-ion oscillation amplitudes along the beam. We see that the longitudinal oscillation wavelength λ_z is somewhat smaller than the beam length: $\lambda_z \approx \frac{2}{3}L_b$.

³⁾This term was proposed by Ya. B. Fainberg.

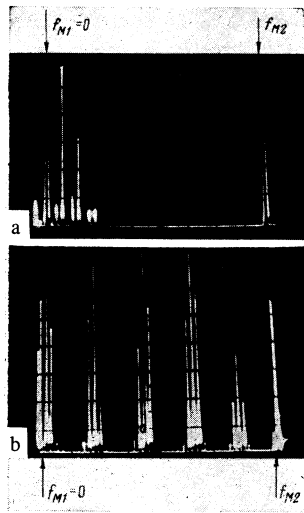


FIG. 10. Spectra of oscillations in a weak magnetic field ($H = 150$ Oe). The arrows indicate the frequency markers: $f_{M1} = 0$, $f_{M2} = 1200$ kHz; $W_1 = 300$ eV; $p = 1.5 \times 10^{-6}$ mm Hg; $L_b = 100$ cm a-I = 5 mA, b-I = 28 mA ($I < I_l$).

Figure 10 shows the frequency spectrum of the oscillations, taken in a weak magnetic field ($H = 150$ Oe). We see that this spectrum consists of harmonics of a certain frequency f_0 . The harmonic content in the oscillation spectrum depends, in particular, on the beam current. (We did not investigate the nature of the low-frequency modulation of the oscillations in question.) In a stronger magnetic field, the spectrum of the oscillations retains the aforementioned singularities, but the "spectral lines" become much broader—Fig. 11. The frequency f_0 is of the order of the Langmuir ion frequency corresponding to the density of the primary beam electrons; when the beam current changes, it varies approximately like $f_0 \propto \sqrt{I}$ (a similar phenomenon was observed by Fedorchenko et al.^[12]).

The foregoing experimental data offer evidence that the spatial structure and the main dispersion properties of the electron-ion oscillations observed in the state II' correspond to the theory^[10] of the drift-beam instability. At the same time, inasmuch as these oscillations are observed not only when $I > I_{cr}$, but also when $I_{exc} < I \ll I_{cr}$ (Fig. 7), the buildup of these oscillations is not hydrodynamic.

According to the theory of^[10], a drift-beam instability can be built up also by a kinetic mechanism, i.e., by resonant particles that move along the magnetic field with velocities v_z that are close to the phase velocity of the wave: in our case $v_z \approx \omega/kz \ll u$, where u is the velocity of the primary beam electrons. Under the conditions of our experiments, such resonant particles are the secondary emission electrons knocked out by the primary electrons from the beam collector. Our experiments have shown that the secondary electrons do indeed play a decisive role in the buildup of electron-ion oscillations in state II'. Thus, when the flux of these electrons is decreased by applying a positive potential on the beam collector located behind a grounded grid, the current I_{exc} at which the electron-ion oscillations begin it is greatly increased; at the same time, the instant when the ions begin to accelerate to high energies

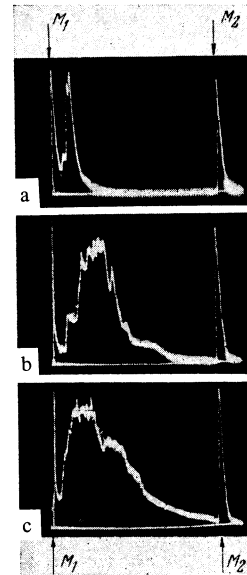


FIG. 11. Spectra of oscillations in a medium magnetic field ($H = 2000$ Oe). The arrows indicate the frequency markers: $f_{M1} = 0$, $f_{M2} = 1200$ kHz; $W_1 = 300$ eV; $p = 2 \times 10^{-6}$ mm Hg; $L_b = 100$ cm. a-I = 8 mA $> I_{exc}$; b-I = 48 mA $> I_{cr}$; c-I $\geq I_l$ (the limiting beam current is $I_l = 53$ mA). a and b pertain to the state II' and c to the state III'.

is correspondingly shifted towards larger beam currents. In the case of a sufficiently large collector potential, the only electrons remaining in the current of the secondary electrons entering into the system are those with sufficiently high energy ("inelastically reflected"), whose distribution function with respect to the longitudinal velocities^[13] has a form similar to a "plateau." These electrons, in accordance with the point of view presented here, are indeed the ones which cause the kinetic buildup of the electron-ion oscillations when $I_{exc} < I < I_{cr}$.

The very existence of a dependence of the current I_{exc} (Fig. 7) on the collector potential V_a can be used to measure the increments of the electron-ion oscillation buildup. To this end it is sufficient to use a potential $+V_a$ at which there are no oscillations ($I_{exc} > I$), apply to the collector a steep negative voltage pulse (thus making the current I_{exc} smaller than the beam current I), and observe the growth of the oscillation amplitude in time. An experiment of this type (so far, preliminary) has shown that the increment of the electron-ion oscillations observed in the state II' is of the same order as the frequency f_0 (or smaller), in agreement with the premises of the theory of^[10] that the oscillation buildup has a kinetic mechanism (in contrast to the hydrodynamic buildup when $I > I_{cr} \approx I_l$, when the increment is much larger than the frequency).

There is one more criterion that distinguishes the conditions of the hydrodynamic and kinetic buildups of the electron-ion oscillations^[10]. According to this criterion, the hydrodynamic buildup is possible only when

$$\frac{n_2}{n_1} < \frac{\omega}{k_z u} \frac{R^2}{a^2}, \quad (5)$$

where a and R are respectively the "radii" of the beam and of the plasma, n_2 is the plasma density, and n_1 is the

density of the primary electrons. For example, if $R \approx a$ and $n_2 \gg n_1$ (as is the case in state I of the plasma beam), then a hydrodynamic buildup of oscillations with frequencies $\omega < k_z u$ is impossible. On the basis of this result, A. B. Mikhaïlovskii predicted, in a private communication, that the transition of a plasma beam from state I directly to state III (with virtual cathode) is impossible. This prediction was confirmed by our experiment (3), in which the "intermediate" state II was observed. In state II we have $R_2 \gg a_2$, and criterion (5) can be satisfied in spite of the fact that $\omega \lesssim k_z u$ (see^[3]); the transition II \rightarrow III is therefore possible as a result of hydrodynamic instability. On the other hand, the transition I \rightarrow III can be effected by kinetic buildup of the oscillations. As is well known^[2,3], this transition takes place under the condition

$$n_1 v_1 > n_2 v_2 / 4, \quad (6)$$

where n_2 and n_1 are respectively the densities of the plasma electrons and of the primary beam, and v_2 and v_1 are their average velocities. This condition agrees qualitatively with the theory of^[10], according to which the increment of the kinetic buildup of the oscillations increases with increasing ratio n_1/n_2 . Since this ratio increases with development of the centrifugal instability of state I, this instability contributes to the start of the kinetic buildup of the electron-ion oscillations, i.e., to the transition I \rightarrow II.

Notice should be taken here of one circumstance that may appear to contradict our point of view. The point is that, according to the theory of^[10], the kinetic buildup of the oscillations should have no threshold with respect to the beam density, thus seemingly contradicting the finite current I_{exc} in the criterion (6). It must be borne in mind, however, that under the experimental conditions there are always several factors which are not taken into account by the theory and which lead to dissipation of the oscillations. For example, the electron-ion waves may not be all standing still throughout the length of the beam, by virtue of which the energy of the oscillations is removed (at the group velocity) from the system; absorbing layers may be located near the electrodes, etc. It is therefore not surprising that intense buildup of the oscillations begins only with a certain beam current, at which the increment of the oscillations exceeds their decrement due to the aforementioned dissipative processes. It is clear from the foregoing that at the present time it is very difficult to calculate the current I_{exc} and to obtain the criterion (6).

Concluding the review of the experimental data pertaining to an electron beam in vacuum, let us turn once more to the acceleration of ions by the electric fields of electron-ion oscillations. These oscillations, as shown by experiment, are not purely harmonic if the magnetic fields are not very weak, and are randomly modulated (as for example, in the case shown in Fig. 11), and therefore the ion acceleration is connected with a stochastic mechanism.

Thus, the aggregate of the experimental data presented here allows us to state that the transitions I \rightarrow II \rightarrow III observed in the plasma beam (similar to the transitions of the quasineutral electron beam I' \rightarrow II' \rightarrow III') are connected respectively with the kinetic and hydrodynamic buildups of axially asymmetrical electron-ion

oscillations, which occur one after the other. In other words, the instabilities which cause the aforementioned transitions and lead, in particular, to the effective acceleration of the ions to high energies, are different manifestations of a rather general drift-beam instability of an inhomogeneous plasma. Under different conditions, namely, when the ratio n_1/n_2 is so small that the drift-beam instability cannot develop in the initial state of the beam, the occurrence of this instability may be greatly enhanced by the development of centrifugal instability, in which the n_1/n_2 ratio increases appreciably^[3]. Under these conditions, the instability of the plasma beam has a three-step character.

3. INFLUENCE OF LONGITUDINAL DENSITY GRADIENT ON THE STABILITY OF THE PLASMA BEAM

The method used in our experiments to produce the plasma beam is connected with the presence of a longitudinal gradient of the pressure p of the neutral gas between the region of the source (where $p = p_1 \approx 10^{-4}$ mm Hg) and the remaining part of the beam (where $p = p_2 \approx 10^{-5}$ mm Hg). An approximately similar situation occurred in the experiments of Neidigh and Weaver^[14], who can be definitely asserted to have dealt with the instability considered above. In accordance with the terminology of (14) the beam can be in two states: "mode I" and "mode II." The first of these states can be identified with state I, and the second apparently with state II. The authors of^[14] have proposed that the instability observed by them ("mode II") is due to the presence of a longitudinal neutral-gas pressure gradient.

In some of our experiments the plasma beam was produced without a longitudinal pressure gradient when the neutral gas (hydrogen, argon, and other inert gases) were admitted not into the source but into the vacuum chamber. Then, in accordance with^[14], only state I was observed; it was impossible to realize the state II (or III) without a longitudinal pressure gradient.

Let us consider the mechanism of this phenomenon. According to condition (6), it is necessary for the transition I \rightarrow II that the ratio n_2/n_1 be smaller than a certain value. But this ratio cannot be too small in the method used to obtain the plasma beam in our experiments. In fact, the method of producing the plasma beam which we used (as well as Vlasov^[6] and Neidigh and Weaver^[14]) was based on igniting the discharge with an incandescent cathode in the plasma source. The ignition of the discharge (abrupt increase of the density of the electron current emitted from the cathode) occurs when an ion layer, on which all the discharge voltage applied to the source is concentrated, is produced at the cathode. The production of such a layer occurs when the Langmuir condition is satisfied^[15]:

$$j_+ / j_e \geq \gamma \sqrt{m/M}, \quad (7)$$

where j_+ is the density of the ion current to the cathode, $j_e = n_1 v_1$ is the density of the electron current from the cathode, and γ is a numerical coefficient that takes into account the details of the distribution of the electric field and the cathode layer and those "initial" velocities with which the plasma electrons enter into the cathode layer. In a low-voltage discharge, according to the

measurements of Langmuir^[15], $\gamma = 1.5-3$. According to the Bohm theory (16)

$$j_+ = 0.4n_+\sqrt{2T_e/M}, \quad (8)$$

where n_+ is the density of the plasma near the cathode layer. According to the more accurate Firsov theory (17)

$$j_+ \approx n_+\sqrt{T_e/4M}. \quad (8')$$

The combination (8) and (8') with (7), with allowance for the fact that $\sqrt{8Te/\pi m} = v_2$, gives the condition (7) for the ignition of the discharge in the form

$$n_+v_2/n_1v_1 \geq 3\gamma. \quad (9)$$

To ascertain whether this condition is compatible with condition (6) for the transition I \rightarrow II, let us consider two different cases.

Case 1. There is no longitudinal ion-density gradient in the plasma column. In this case the density n_+ of the ions near the cathode layer of the source is equal to the density n_2 of the ions outside the source. The conditions (9) and (6) are then compatible if

$$3\gamma < n_2v_2/n_1v_1 < 4, \quad (10)$$

which is impossible, since $\gamma = 1.5-3$. Consequently, if the discharge takes place in the source of the plasma beam, then the transition I \rightarrow II is impossible.

Case 2. There is an appreciable longitudinal density gradient in the plasma column. With this, $n_+ \gg n_2$, and simultaneous satisfaction of the conditions (6) and (9) is greatly facilitated. In this case the plasma beam can be in state II.

Under real experimental conditions (Fig. 1) the longitudinal plasma-density gradient takes place if the gas is fed to the source, and is due in this case to the presence of a longitudinal neutral-gas density gradient. If the gas is fed to the vacuum chamber, then there is no longitudinal plasma-density gradient. This explains why it is impossible to realize states II and III in the absence of a pressure drop between the source and the vacuum chamber.

To make this conclusion more understandable, let us turn again to the experimental conditions. Let the plasma beam be in state I and let us gradually decrease the flow of the gas into the apparatus. Then, regardless of the presence or absence of a longitudinal pressure gradient in the gas, the plasma density will decrease. In the absence of a longitudinal gas pressure gradient, this causes the discharge to become extinguished before the plasma density drops to a value corresponding to the condition for the transition I \rightarrow II. In other words, in a discharge without a longitudinal gas pressure gradient, the transition I \rightarrow II "has no time" to occur, since the discharge is extinguished earlier. In the presence of a longitudinal gas pressure gradient, the transitions I \rightarrow II \rightarrow III will be realized so long as the discharge still takes place.

If another method, not connected with formation of a Langmuir double layer at the cathode, were to be used to obtain the plasma beam, then the beam could be in states II and III even in the absence of a longitudinal gas pressure gradient. It is easy to see that this conclusion

agrees with the experimental data presented in Sec. 2 (Figs. 7 and 8) and illustrating the existence of states II' and III' in the absence of a longitudinal gas pressure gradient, when condition (9) for the ignition of the discharge is satisfied, and an electron beam of sufficient density is produced with the aid of an accelerating grid placed over that edge of the discharge chamber of the source which faces the cathode.

The author is grateful to Ya. B. Faĭnberg, M. S. Ioffe, and B. B. Kadomtsev for a discussion of the results, and S. A. Vol'nov and M. I. Taktakishvili for taking part in the experiments.

¹M. V. Nezlin, Zh. Eksp. Teor. Fiz. 41, 1015 (1961) [Soviet Phys.-JETP 14, 723 (1962)]; ibid. 46, 36 (1964) [19, 26 (1964)].

²M. V. Nezlin and A. M. Solntsev, ibid. 45, 840 (1963) [18, 576 (1964)]; ibid. 48, 1237 (1965) [21, 826 (1965)].

³M. V. Nezlin and A. M. Solntsev, ibid. 49, 1377 (1965) [22, 949 (1966)].

⁴L. A. Artsimovich, Upravlyaemye termoyadernye reaktzii (Controlled Thermonuclear Reactions), Fizmatgiz, 1963; A. A. Vedenov, E. P. Velikhov, and R. Z. Sagdeev, Usp. Fiz. Nauk 73, 701 (1961) [Soviet Phys.-Usp. 4, 332 (1961)].

⁵E. P. Velikhov, Zh. Tekh. Fiz. 31, 180 (1961) [Soviet Phys.-Tech. Phys. 6, 130 (1961)].

⁶M. A. Vlasov, ZhETF Pis. Red. 2, 274 (1965) [JETP Lett. 2, 174 (1965)].

⁷M. F. Gorbatenko and V. D. Shapiro, in: Vzaimodeĭstvie puchkov zaryazhennykh chastits s plazmoĭ (Interaction of Charged-particle Beams with a Plasma), AN UkrSSR, Kiev, 1965, p. 103.

⁸M. N. Rosenbluth and A. Simon, Phys. Fluids 8, 1300 (1965).

⁹M. V. Nezlin and A. M. Solntsev, Zh. Eksp. Teor. Fiz. 53, 437 (1967) [Soviet Phys.-JETP 26, in press].

¹⁰A. B. Mikhaĭlovskii, Zh. Tekh. Fiz. 35, 1945 (1965) [Soviet Phys.-Tech. Phys. 10, 1498 (1966)]; Atomnaya ėnergiya 20, 103 (1966).

¹¹E. A. Lovetskiĭ and A. A. Rukhadze, Nuclear Fusion 6, 9 (1966); L. S. Bogdankevich and A. A. Rukhadze, ibid. 6, 176 (1966).

¹²V. D. Fedorchenko, B. N. Rutkevich, V. I. Muratov, and B. M. Chernyi, Zh. Tekh. Fiz. 32, 958 (1962) [Soviet Phys.-Tech. Phys. 7, 696 (1963)].

¹³H. Bruining, Physics and Applications of Secondary Electron Emission, Pergamon, 1954.

¹⁴R. V. Neidigh and C. H. Weaver, Proc. 2-nd Intern. Conf. on Peaceful Uses of Atomic Energy, 31, Report 2396, Geneva, 1958, p. 315.

¹⁵J. Langmuir, Phys. Rev. 33, 954 (1929).

¹⁶D. Bohm, The Characteristics of Electrical Discharges in Magnetic Fields, N. Y., 1949.

¹⁷O. B. Firsov, Zh. Tekh. Fiz. 26, 445 (1956) [Soviet Phys.-Tech. Phys. 1, 431 (1956)].